



*Supplement of*

## **Western boundary circulation and coastal sea-level variability in Northern Hemisphere oceans**

**Samuel Tiéfolo Diabaté et al.**

*Correspondence to:* Samuel Tiéfolo Diabaté ([samuel.diabate.2020@mumail.ie](mailto:samuel.diabate.2020@mumail.ie))

The copyright of individual parts of the supplement might differ from the article licence.

**Table S1.** The Atlantic tide gauges used in the study, with their locations (approximate) and completeness before interpolation is applied. The angle used to rotate winds in an alongshore/across-shore coordinate system are also shown.

No.	Station	PSMSL ID	Longitude (°E)	Latitude (°N)	Completeness <sup>a</sup> (%)	Angle <sup>b</sup> (°)
1	Key West	188	-81.807	24.555	98.8	0
2	Fernandina Beach	112	-81.465	30.672	96.4	111
3	Fort Pulaski	395	-80.902	32.033	98.6	42
4	Charleston I	234	-79.925	32.782	100.0	42
5	Wilmington	396	-77.953	34.227	98.3	42
6	Sewells Point, Hampton Roads	299	-76.330	36.947	100.0	65
7	Washington DC	360	-77.022	38.873	97.9	65
8	Solomon's Island (Biol. Lab.)	412	-76.452	38.317	95.7	65
9	Annapolis (Naval Academy)	311	-76.480	38.983	95.4	65
10	Baltimore	148	-76.578	39.267	99.7	65
11	Lewes (Breakwater Harbor)	224	-75.120	38.782	95.7	65
12	Philadelphia (Pier 9N)	135	-75.142	39.933	97.7	65
13	Atlantic City	180	-74.418	39.355	92.6	65
14	Sandy Hook	366	-74.008	40.467	98.5	65
15	New York (The Battery)	12	-74.013	40.700	98.8	65
16	Montauk	519	-71.960	41.048	92.0	65
17	New London	429	-72.090	41.360	96.2	65
18	Newport	351	-71.327	41.505	98.7	65
19	Woods Hole (Ocean. Inst.)	367	-70.672	41.523	93.6	65
20	Boston	235	-71.053	42.353	98.7	21
21	Portland (Maine)	183	-70.247	43.657	99.7	21
22	Eastport	332	-66.982	44.903	92.2	21

<sup>a</sup>Completeness is computed over the period 1948 – 2019 for the Atlantic gauges.

<sup>b</sup>Coastline angles are approximate and measured counterclockwise from east.

**Table S2.** Same as the previous table, but for the Pacific set of tide gauges.

No.	Station	PSMSL ID	Longitude (°E)	Latitude (°N)	Completeness <sup>a</sup> (%)	Angle <sup>b</sup> (°)
1	Odomari	1097	130.689	31.024	99.2	85
2	Aburatsu	814	131.409	31.577	100.0	85
3	Hosojima	133	131.669	32.429	96.5	85
4	Tokuyama II	1210	131.803	34.041	100.0	19
5	Tosa Shimizu	815	132.959	32.779	100.0	19
6	Matsuyama II	1062	132.712	33.859	98.4	19
7	Hirosima	1028	132.465	34.353	98.7	19
8	Kure IV	1209	132.550	34.241	99.0	19
9	Uno	812	133.949	34.489	96.6	19
10	Komatsushima	809	134.588	34.009	98.7	19
11	Sumoto	1098	134.907	34.341	98.9	19
12	Shirahama	1150	135.375	33.684	98.9	19
13	Kainan	701	135.191	34.144	99.0	19
14	Wakayama	816	135.146	34.222	99.8	19
15	Tan-Nowa	817	135.178	34.339	97.9	19
16	Kushimoto	134	135.773	33.476	98.6	19
17	Uragami	1090	135.896	33.558	96.2	19
18	Owase	1146	136.207	34.076	93.9	19
19	Shimizu-Minato	808	138.518	35.012	99.7	19
20	Uchiura	407	138.890	35.017	99.0	19
21	Okada	1091	139.391	34.789	99.2	19
22	Aburatsubo	130	139.615	35.160	99.0	19
23	Yokosuka	722	139.651	35.288	99.5	19
24	Katsuura	1191	140.249	35.129	97.9	19
25	Onahama <sup>c</sup>	635	140.892	36.938	99.7	100
26	Ayukawa <sup>c</sup>	131	141.505	38.297	98.4	100
27	Asamushi	721	140.859	40.898	98.9	100
28	Miyako II <sup>c</sup>	1149	141.975	39.643	99.8	100
29	Hakodate I	813	140.725	41.782	99.5	100
30	Kushiro	518	144.371	42.976	99.5	20

<sup>a</sup>Completeness is computed over the period 1968 – 2019 for the Pacific gauges.

<sup>b</sup>Coastline angles are approximate and measured counterclockwise from east.

<sup>c</sup> Timeseries that were filled with SSH from 2011 onwards.

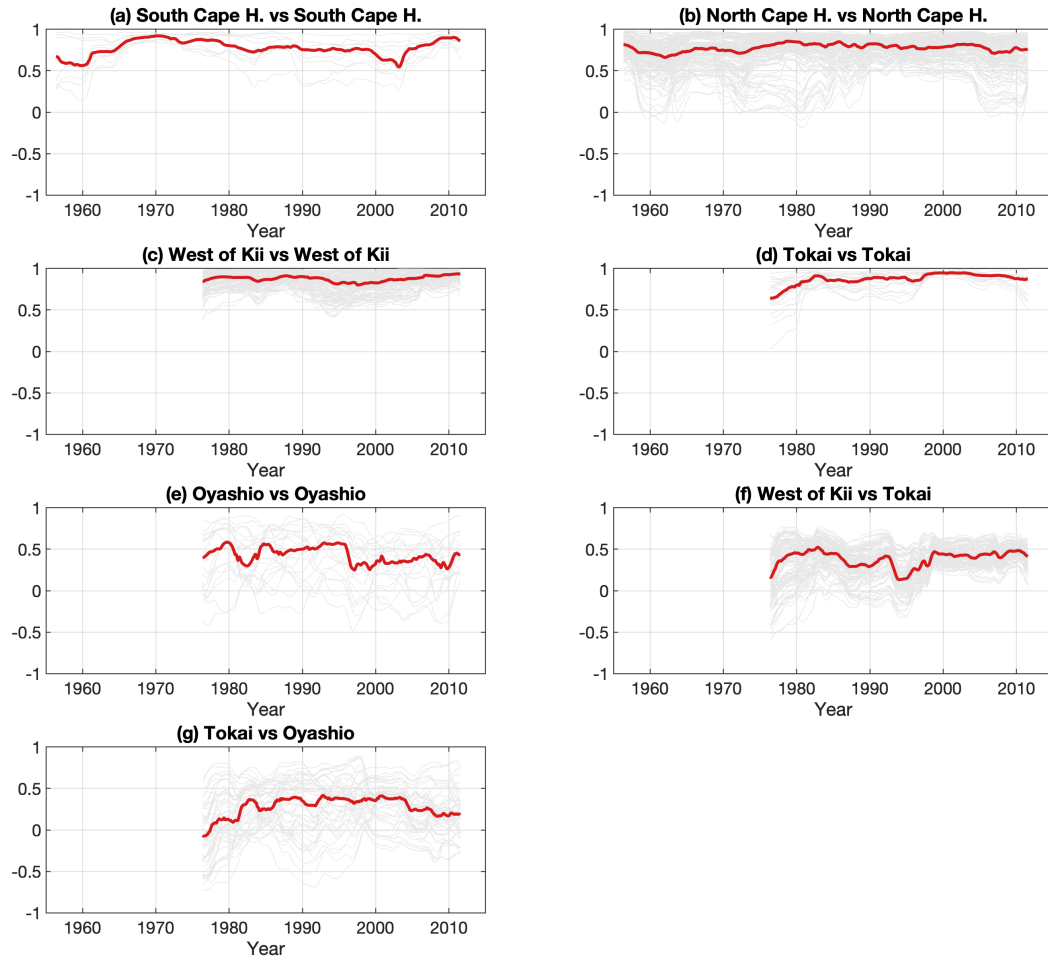


**Figure S1.** Moving correlation analysis between the tide gauges records with a running window of 15 years. Each individual grey line renders the moving correlation between two records. The x-axis represents the center of the moving window. (a) Cross-correlation between gauges located south of Cape Hatteras. (b, c, d, and e) as in (a), but for gauges north of Cape Hatteras (b), west of Kii (c), south of Tōkai (d), and (e) east of Honshū–Hokkaidō (*i.e.*, the Oyashio group) respectively. (f) Cross-correlation uniquely between gauges on either side of the Kii peninsula (west of Kii versus south of Tōkai). (g) as (f), but for the groupings south of Tōkai and the Oyashio group. On each panel, the solid thick red line is the median of the individual cross-correlations.

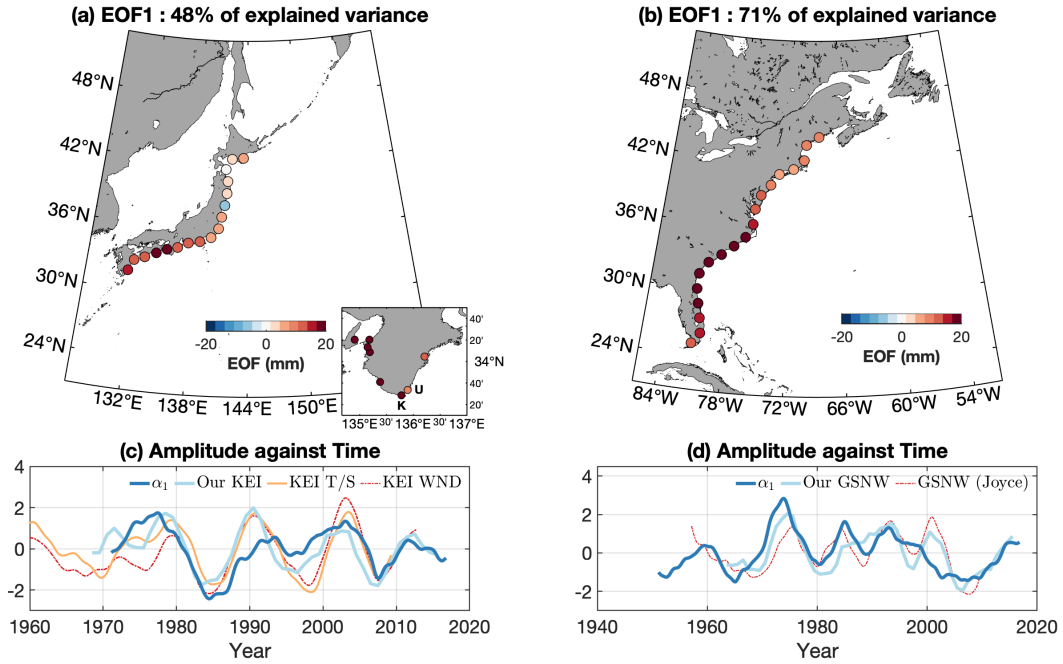


**Figure S2.** (a) and (b) present the leading EOF ( $\phi_1$ ) of the 73-months filtered sea-level anomaly obtained with the Pacific gauges and the Atlantic gauges respectively (circular markers). (c) and (d) present, for the Pacific and Atlantic respectively, the associated principal components  $\alpha_1$  (solid blue lines), together with indices of extension meridional location: this study and Qiu et al. (2016) T/S-based and wind-based KEIs (on (c), thick light blue line, orange solid line and dot-dashed red line respectively); and this study and Joyce et al. (2000) GSNWs (on (d), thick light blue line and dot-dashed red line, respectively). All quantities on (c) and (d) are normalized. On (c), it is apparent that the variations of  $\alpha_1$  between 1998 and 2005 are now joined into one single lobe due to the filtering. The inset on (a) present the regression coefficient obtained when the principal component is regressed on the original tide gauges, with a zoom in on the Kii peninsula.

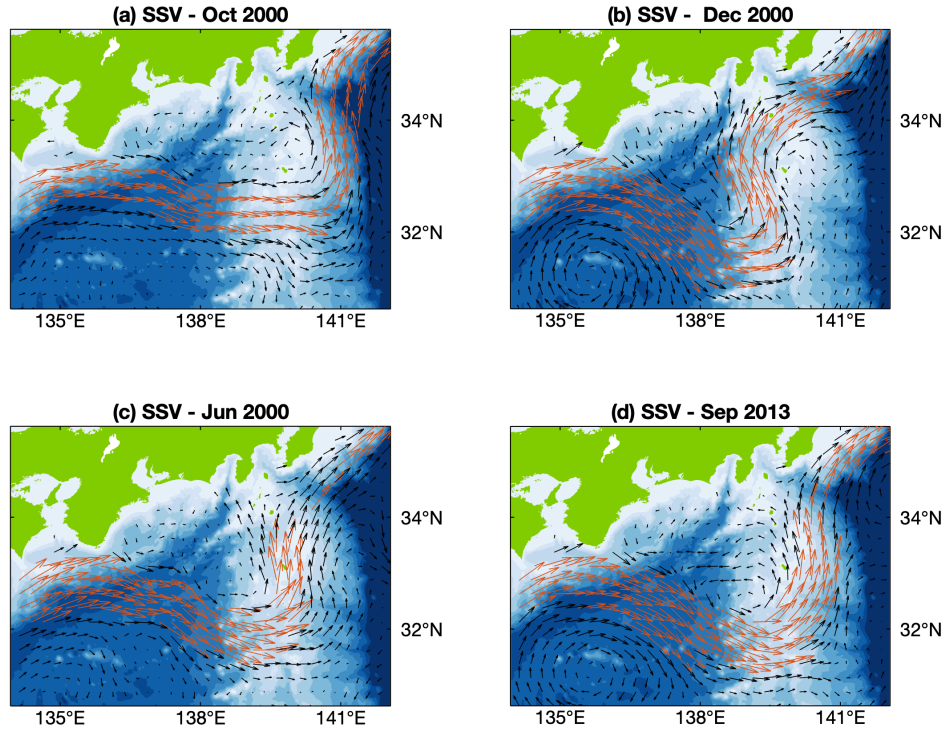


**Figure S3.** Situation during the two recent periods of strong positive  $\alpha_2$  that are not concurrent to tLM: April 2000 to April 2001, and the second half of 2013. (a), (b) (c) and (d) are snapshot of the velocities for December 2000, October 2000, June 2000 and September 2013, respectively. Between April 2000 and April 2001, the Kuroshio alternated between unusual offshore NLM similar to the October 2000 snapshot presented on (a), non-persistent typical LM of one or two months lifetime, as on (b), and situations somewhat in between where the Kuroshio follows the ridge, as on (c). Large velocity vectors (in orange) were clipped to highlight the westward current nearshore in the area 137°E – 140°E, 33°N – 34.5°N. For this particular panel SSV were not 19-months filtered.

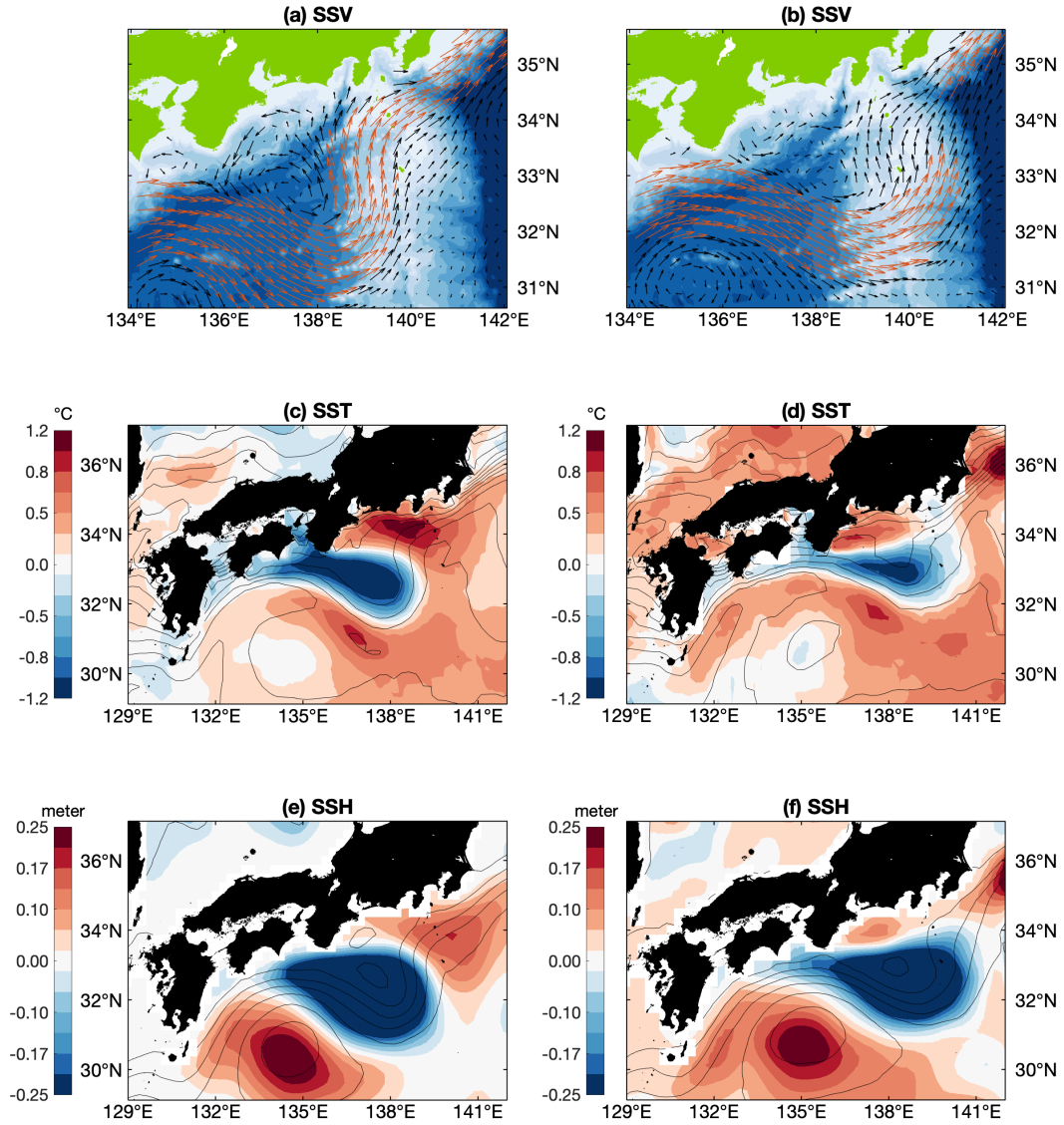


**Figure S4.** (a) SST, (c) SSH and (e) surface velocities averaged over the period of typical large meander during the satellite era (JMA, 2018). Black contours represent the average over the large meander periods and shadings the deviation from the 1993–2020 mean. Akin figures can be found in Sugimoto et al. (2019) (a and c), and Usui et al. (2013) (e). (b – f) are similar to (a – e), but averaged over April 2000 – April 2001 rather than over typical large meander periods. In (a) and (b), large velocity vectors (in orange) were clipped to highlight the westward current nearshore in the area 137°E – 140°E, 33°N – 34.5°N. For this particular panel, SST, SSV and SSH were not 19-months filtered.

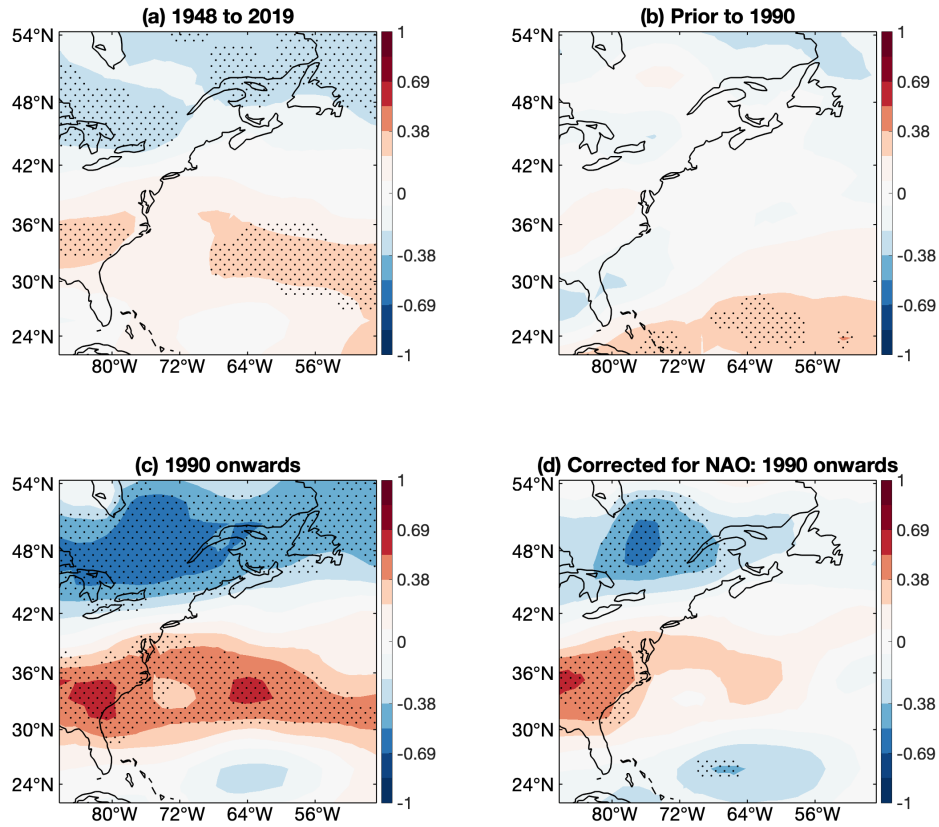


**Figure S5.** Correlation between the wind stress projected onto a  $20^\circ$  from zonal angle and the principal component  $\alpha_2$ , on the period (a) 1948 – 2019, (b) 1948 – 1989 and (c) 1990 – 2019. (d) shows the correlation for the period 1990 – 2019 corrected for the NAO variations (the so-called partial correlation). The monthly NAO is used instead of DJFM NAO, for compatibility with winds and  $\alpha_2$ . Dotted areas represent significant correlations at 5% significance level.



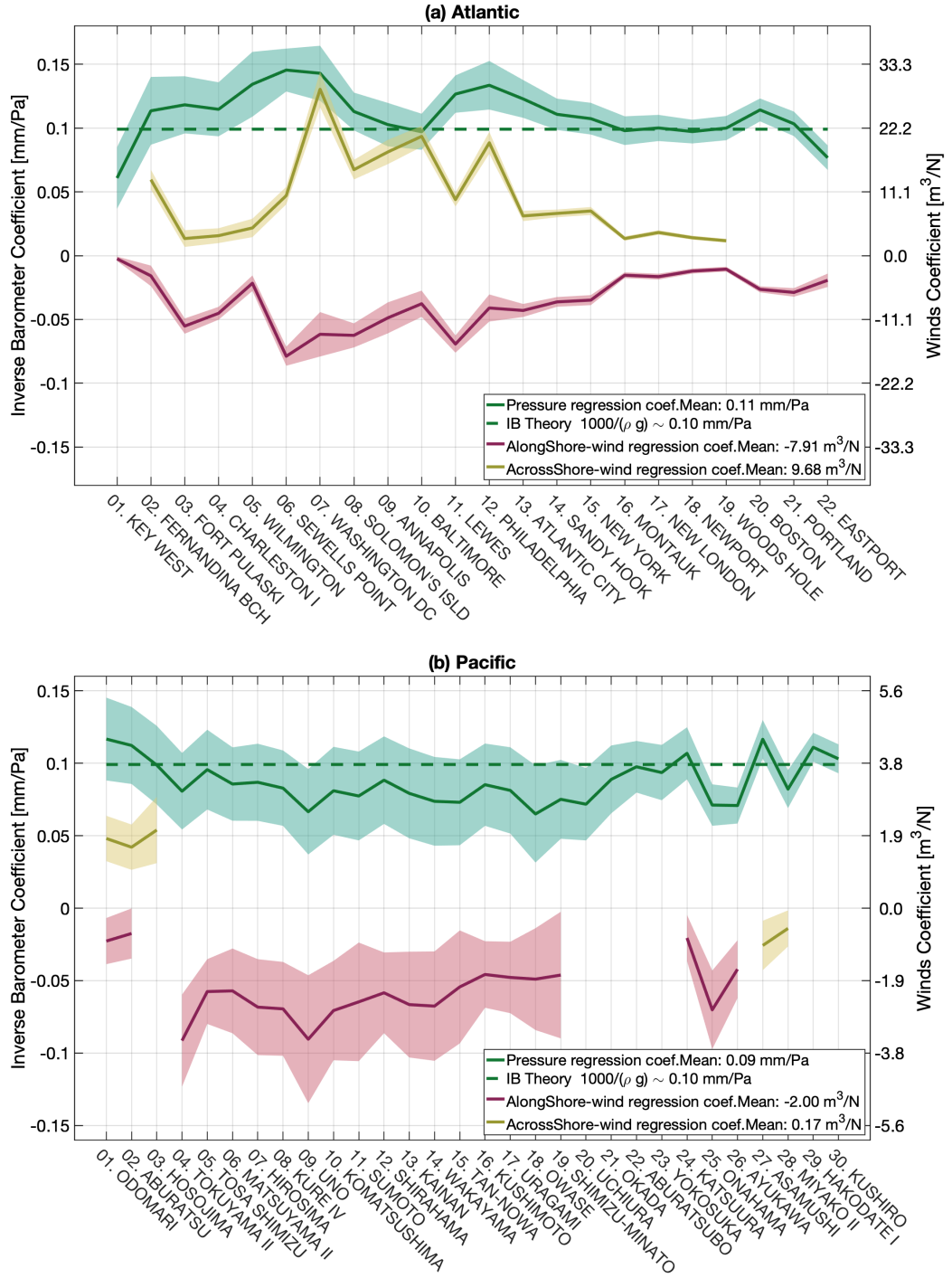


**Figure S6.** Regression coefficients of the pressure (solid green line) and alongshore and across-shore windstress (respectively red and yellow lines) obtained for (a) Atlantic and (b) Pacific gauges. Shadings indicate the confidence intervals. For each tide gauge, only the regression coefficients of the best subset regression are shown. The expected inverse barometer response is, in theory,  $(\rho g)^{-1} \sim 0.10 \text{ mm/Pa}$  and is also shown (dashed dark green line). Note that for the tide gauge of Key West, the windstress is not rotated,  $\phi = 0$ :  $\tau_u$  and  $\tau_v$  are used as regressors.

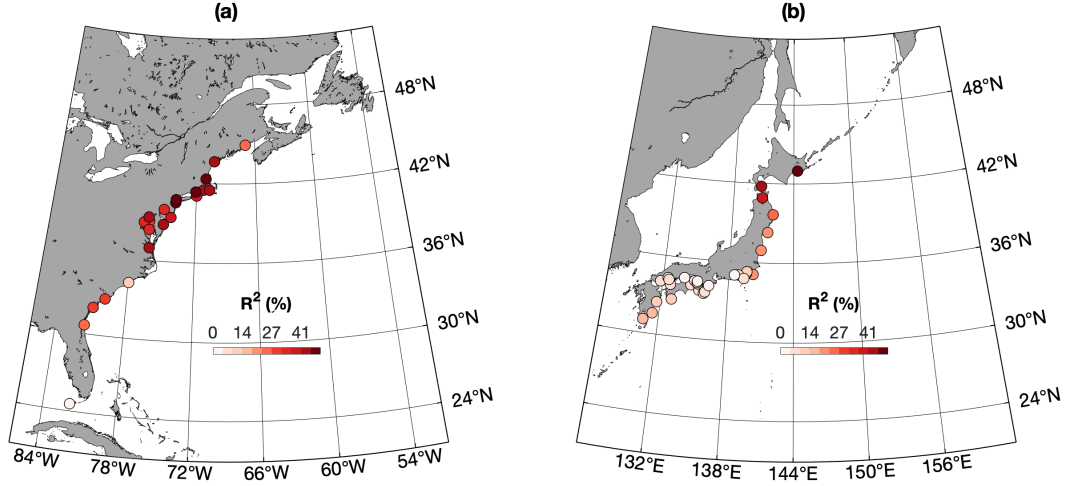


**Figure S7.** The adjusted coefficient of determination  $R^2_{Adj}$  obtained for the (a) Atlantic and (b) Pacific gauges. This quantity indicates how much does the best subset regression explain of the monthly sea level.

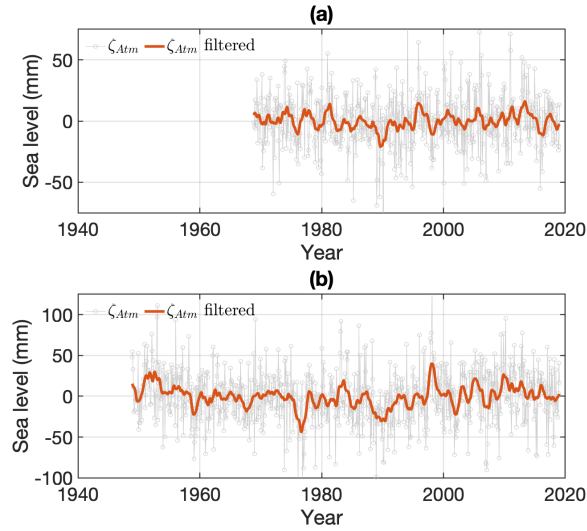


**Figure S8.** Average over the stations (a) east of Honshū–Hokkaidō (*i.e.*, the Oyashio group in the Pacific) and (b) north of Cape Hatteras (Atlantic) of the component  $\zeta_{Atm}$  that is removed from the tide gauge records to correct for local atmospheric forcing. Thick orange line is  $\zeta_{Atm}$  after a 19-months filter is applied.